



## Article Info

Received: 27<sup>th</sup> October 2024Revised: 3<sup>rd</sup> December 2024Accepted: 10<sup>th</sup> December, 2024<sup>1</sup>Department of Mathematics, Sokoto State University, Sokoto, Nigeria.<sup>2</sup>Department of Physics, Sokoto State University, Sokoto, Nigeria

\*Corresponding author's email:

[abdulahihussaini6@gmail.com](mailto:abdulahihussaini6@gmail.com)Cite this: *CaJoST*, 2025, 1, 150-161

## Mixed Convection Flow of an Electrically Conducting Viscoelastic Fluid Between Vertical Parallel Plates: Insights on Thermal Radiation, Heat Source/Sink, and Dissipation Effects

Hussaini Abdullahi<sup>1</sup>, Sahabi Z. Yabo<sup>1</sup> and Anas Shehu<sup>2</sup>

This study explores the mixed convection boundary layer flow and heat transfer of a viscoelastic fluid across a parallel plate, considering the influence of an applied magnetic field, thermal radiation, and viscous dissipation. The equations governing the flow of the fluid are described as Partial Differential Equations (PDEs) and Finite Difference Method (FDM) is used to obtain numerical solutions. Numerical investigations were conducted to examine the effect of parameters in the flow of the fluid i.e. on the velocity, temperature and concentration with the aid of graphs. Efficient heat transfer is critical in designing heat management systems for various industrial applications, where the heat transfer rate may need to be increased or decreased to optimize heating or cooling processes. Additionally, the findings are significant because the wall material's thermal properties depend on the cooling or heating rates during the production of metal or polymer sheets. Radiative effects and viscous dissipation contribute to higher temperature distributions and the expansion of the thermal boundary layer. Radiation particularly enhances heat generation in fluids, increasing their temperature, especially at elevated temperatures where it directly impacts heat transfer and temperature distribution. In the boundary layer, where transport phenomena oppose each other, the magnetic field becomes the dominant factor. The study further demonstrates that an applied magnetic field increases the fluid temperature profile while reducing the rate of heat transfer through the walls.

**Keywords:** Viscoelastic fluid; Magnetohydrodynamic (MHD); Thermal radiation; Heat source/sink; Viscoelastic fluid.

## 1. Introduction

Researchers are drawn to studying fluids due to their widespread applications across various fields of science and technology. Fluid dynamics, a critical subset of fluid mechanics, focuses on understanding the movement of fluids. The three key conservation laws governing fluid flow include the conservation of mass, momentum, and energy. Fluids are typically classified into two major categories: Newtonian and non-Newtonian fluids. For Newtonian fluids, the relationship between stress and strain rate is linear. In contrast, non-Newtonian fluids do not adhere to Newton's law of viscosity, exhibiting a nonlinear connection between stress and strain rate. This results in highly nonlinear governing equations. Despite extensive research, there is no single model in the literature that fully encapsulates all the characteristics of non-Newtonian fluids. Non-Newtonian transport phenomena can be observed in various industries, such as mining, food processing, printing, and the chemical sector, thereby motivating

new researchers to delve into the study of these fluids.

Thermal radiation represents a method of heat transfer that involves the emission of heat energy by liquid particles. This process is crucial in designing energy systems that operate at high temperatures, such as nuclear power plants, polymer processing units, satellites, gas turbines, spacecraft, and missiles. For instance, Makinde (2005) analyzed free convection involving radiation on a vertical porous surface, while Hayat *et al.* (2010) studied the effects of thermal radiation and Magnetohydrodynamic (MHD) on mixed convection at a stagnation point past a vertical stretched sheet. Similarly, Mukhopadhyay *et al.* (2011) explored the heat transfer and steady boundary layer flow over a porous moving plate in the presence of thermal radiation. Heat generation within a body, such as air movement due to sunlight absorption, commonly

leads to natural convection. Das (2012) examined the impact of partial slip, thermal radiation, and a non-uniform heat source/sink on MHD flow over a flat plate, while Pramanik (2014) focused on Casson fluid flow and heat transfer over an exponentially porous stretched sheet. Additionally, Kataria *et al.* (2016) discussed the influence of heat generation and thermal diffusion on MHD Casson fluid flow in porous media. Sheikholeslami *et al.* (2016) and Sulochana *et al.* (2016) investigated the thermophoretic and Brownian motion effects on MHD Nano fluid flow, with further studies by Kumaran *et al.* (2017) addressing similar phenomena for Casson and Williamson fluids. Many other researchers Sulochana *et al.* (2016), Mythili and Sivaraj (2016), Ghiasi and Saleh (2019), Prasad *et al.* (2019) have analyzed MHD Casson fluid flow with varying geometries, accounting for non-uniform heat sources/sinks. Yasir *et al.* (2021), (2023) explored flow and heat transfer in Oldroyd-B fluids with nanoparticles, contributing to the understanding of MHD systems.

Viscoelastic fluids represent a unique category of non-Newtonian fluids that exhibit both viscosity and elasticity. This dual behavior makes them essential in various applications, such as heat transfer reduction and drag reduction, particularly in the polymer industry. They are widely utilized in the production of paper, fiberglass, dyes, films, synthetic fibers, and plastic sheets, as well as in cooling metallic chips and food processing. Viscoelastic fluids also play a significant role in oil reservoir engineering, bioengineering, the chemical industry, and nuclear technology. The behavior of viscoelasticity affects the rate of heat transfer, depending on the velocity field being studied and the direction of heat exchange. Researchers such as Abel (2001) have examined heat transfer in electrically conducting viscoelastic fluid flows induced by non-isothermal stretching surfaces, finding that increased viscoelasticity reduces temperature distributions within the boundary layer. Sivaraj and Kumar (2013) also explored the free conductive flow of Walters' B viscoelastic fluid over flat plates and vertical cones, discovering that variations in electric conductivity and magnetic fields significantly influence viscoelastic flow. Additionally, Maryam *et al.* (2020) achieved numerical solutions for viscoelastic fluids using a second-order parallelized finite volume method, highlighting that the drag coefficient at the boundary of viscoelastic fluids is lower than that of Newtonian fluids. Further theoretical studies, such as those by Cortell (2013), demonstrated that the viscosity of second-grade viscoelastic fluids is greater than that of Walters' B fluid, with similar investigations by Mustapha (2016) employing homotopy analysis to explore nonlinear stretching sheets.

Radiation, the emission of energy in the form of electromagnetic waves, also plays a critical role in fluid dynamics, particularly in altering fluid parameters during flow. The thermal radiation effect is essential for controlling system temperatures, adjusting heat transport rates, and managing the thermal boundary layer. For instance, Kumaran *et al.* (2000) studied the effect of thermal radiation on natural convective Powell-Eyring Nano fluid flow, concluding that an increase in the radiation parameter reduces heat transfer. Several other studies Sheikholeslami *et al.* (2016), Mythili and Sivaraj (2016), and Abel (2001) have explored the impact of radiant heat on boundary layer flow driven by a nonlinearly stretching sheet due to its significance in maintaining system temperatures. In addition to thermal radiation, the effects of viscous dissipation a process where friction between fluid layers generates heat must be considered. This energy source modifies temperature distributions, impacting heat transfer rates.

The primary objective of this study is to obtain a numerical solution for viscoelastic fluid flow under the combined influence of a uniform magnetic field, viscous dissipation, and thermal radiation over a vertical parallel plate. By employing an unconditionally stable finite difference technique to solve a system of nonlinear partial differential equations, non-similar solutions are computed numerically, a method previously utilized by researchers like Kumaran *et al.* (2017) and Hayath *et al.* (2010).

## 2. Mathematical formulation of the problem

We take into account a viscoelastic fluid flowing in mixed convective two-dimensional Magnetohydrodynamic flow across upright parallel plate. The  $x$ -axis is drawn along the continuously extending surface and faces forward. The sheet is parallel to the  $y$ -axis. The plate is subjected to a perpendicular magnetic field. The plate velocity, is assumed to vary as a nonlinear function of the distance from the slit, the temperature of the fluid, is also considered as a nonlinear function of the distance from the slit, where  $T_0$  a positive constant is and  $T_h$  is the ambient temperature of the fluid.

Thus, using the conventional boundary layer approximation, the viscoelastic fluid equations governing continuity, the momentum, energy and concentration equations may be expressed as follows equations (1)-(4)

The continuity equation

$$\frac{\partial v^*}{\partial y^*} = 0$$

(1)

The momentum equation

$$\frac{\partial u^*}{\partial t^*} + v^* \frac{\partial u^*}{\partial y^*} = g \left[ \beta(T^* - T_0) + \beta(C^* - C_0) \right] + \nu \frac{\partial^2 u^*}{\partial y^{2*}} + \beta_1 \left[ \frac{\partial^3 u^*}{\partial t^* \partial y^{2*}} - \nu \frac{\partial^3 u^*}{\partial y^{3*}} \right] - \dots$$

$$\nu \frac{u^*}{k} - \frac{\sigma \mu e^2 H_0^2}{\rho} u^*$$
(2)

The energy equation

$$\frac{\partial T^*}{\partial t^*} + v^* \frac{\partial T^*}{\partial y^*} = \frac{k}{\rho C_p} \frac{\partial^2 T^*}{\partial y^{2*}} + \frac{Q}{\rho C_p} (T^* - T_0) - \frac{1}{\rho C_p} \left( \frac{\partial q}{\partial y} \right) + \frac{\mu}{C_p} \left( \frac{\partial u^*}{\partial y^*} \right)^2$$
(3)

The concentration equation

$$\frac{\partial C^*}{\partial t^*} + v^* \frac{\partial C^*}{\partial y^*} = D \frac{\partial^2 C^*}{\partial y^{2*}} - k_r^* (C^* - C_0)^n$$

(4)

The approve boundary condition to the problem for concentration, temperature and velocity fields are:

$$t^* \leq 0: u^* = 0, T^* = T_h, C^* = C_h \text{ for } y^* \leq H$$

$$t^* > 0: \left. \begin{array}{l} u^* = 0, T^* = T_w, C^* = C_w \text{ at } y^* = 0 \\ u^* = 0, T^* = T_h, C^* = C_h \text{ at } y^* = H \end{array} \right\}$$

(5)

whereas  $u^*, v^*$  are the velocity component in  $x, y$  directions respectively,  $t^*$  - the time,  $g$  - the acceleration due to gravity,  $\beta$  - the volumetric coefficient of thermal expansion,  $\beta^*$  - the volumetric coefficient of expansion with concentration,  $T^*$  - the temperature of the fluid in the boundary layer,  $C^*$  - the species concentration in the boundary layer,  $\nu$  - the kinematic viscosity,  $\sigma$  - the electrical conductivity,  $B_0$  - the magnetic induction,  $\rho$  - the density of the fluid,  $C_p$  - the specific heat at constant pressure,  $q_r$  - the radiation heat flux,  $Q_0$  - the heat generation/absorption,  $D$  - the species diffusion concentration, and  $n$  - chemical reaction order.

In order to ascertain that the generated magnetic field is minimum, it is also anticipated that the liquid has weak electrical conductivity. The heat flux is adopted to be proportionate to the temperature difference in this approximation, and heat moves from the hard surface to the liquid. In light of this, the radiative heat flux  $q_r$  under Rosseland estimation by Brewster M.Q () is given in the following form:

$$q_r = -\frac{4\sigma_0^*}{3k^*} \frac{\partial T'^4}{\partial y'}$$

(6)

Whereas  $\sigma_0^*$  signifies Stefan-Boltzmann constant and  $k^*$  symbolizes the rate. Adopting that  $T'^4$  can be represented as a linear function of temperature can be expressed as linear function of the temperature as

$$T'^4 = 4T_\infty'^3 T' - 3T'^4$$

(7)

Utilizing Eqns. (7) and (8) into Eqn. (3) to obtain

$$\frac{\partial T^*}{\partial t^*} + v^* \frac{\partial T^*}{\partial y^*} = \left( \frac{k}{\rho C_p} \right) \frac{\partial^2 T^*}{\partial y^{2*}} + \frac{1}{\rho C_p} \frac{16T_\infty'^3 \sigma_0^*}{3k^*} \frac{\partial^2 T^*}{\partial y^{2*}} + \frac{\mu}{C_p} \left( \frac{\partial u^*}{\partial y^*} \right) + \frac{Q_0}{\rho C_p} (T^* - T_h^*)$$
(8)

It is required to make Eqs (2), (9) and (4) dimensionless for this reason we introduce the given dimensionless quantities:

$$\left. \begin{aligned} y &= \frac{y^*V_0}{\nu}, t = \frac{t^*V_0^2}{4\nu}, u = \frac{u^*}{V_0}, \theta = \frac{T^* - T_0}{T_w - T_0}, \phi = \frac{C^* - C_0}{C_w - C_0} \\ Gr &= \frac{\nu g \beta (T_w - T_0)}{V_0^2}, Pr = \frac{\mu C_p}{k}, k = \frac{k^*V_0^2}{k}, M = \frac{\sigma \mu e^2 H_0^2 \nu}{\rho V_0^2} \\ Rm &= \frac{\beta_1 V_0^2}{\nu^2}, Gc = \frac{\nu g \beta^* (C_w - C_0)}{V_0^2}, Sc = \frac{\nu}{D} \end{aligned} \right\}$$

(9)

The following equations and boundary condition are received:

$$\frac{\partial u}{4\partial t} - \frac{\partial u}{\partial y} = \frac{\partial^2 u}{\partial y^2} + Rm \left\{ \frac{\partial^3 u}{4\partial t \partial y^2} - \frac{\partial^3 u}{\partial y^3} \right\} + Gr\theta + GcC - \left( \frac{1}{k} + M \right) u$$

(10)

$$Pr \left[ \frac{\partial \theta}{4\partial t} - \frac{\partial \theta}{\partial y} \right] = \frac{\partial^2 \theta}{\partial y^2} - R\theta + Pr\phi\theta + Pr Ec \left( \frac{\partial u}{\partial y} \right)^2$$

(11)

$$Sc \left[ \frac{\partial C}{4\partial t} - \frac{\partial C}{\partial y} \right] = \frac{\partial^2 C}{\partial y^2} - KrC^n$$

(12)

And the corresponding starting and boundary conditions are:

$$t > 0: \left. \begin{aligned} u &= 0, \theta = 1, C = 1 \text{ at } y = 0 \\ u &= 0, \theta = 0, C = 0 \text{ at } y = 1 \end{aligned} \right\}$$

(13)

Where  $Rm$  is the viscoelastic parameter,  $Gr$  is the thermal Grashof number,  $Gc$  is the solutal Grashof number,  $M$  is the magnetic parameter,  $R$  is the radiation parameter,  $\phi$  is the dimensionless heat generation/absorption coefficient,  $Pr$  is the Prandtl number,  $Ec$  is the Eckert number,  $Sc$  is the Schmidt number and  $Kr$  is the chemical reaction parameter.

### 3. Numerical Solution

Equations (10)-(12) with boundary conditions (13) are solved numerically employing implicit finite difference scheme. Forward difference expressions

$$-r_1 u_{i-1}^{j+1} + (1 + 2r_1 - ARm)_i^{j+1} - r_1 u_{i+1}^{j+1} = (r_2 + r_4) u_{i-1}^j + \left( 1 - r_3 - 2r_2 + ARm - 3r_4 - \frac{4\Delta t}{k} - 4\Delta t M \right) u_i^j + \dots$$

$$(r_1 + r_3 + 4r_4) u_{i+1}^j + r_4 u_{i+2}^j + 4\Delta t Gr \theta_i^j + 4\Delta t Gc C_i^j$$

(14)

$$-r_1 \theta_{i-1}^{j+1} + (Pr + 2r_1) \theta_i^{j+1} - r_1 \theta_{i+1}^{j+1} = r_2 \theta_{i-1}^j + (Pr - r_3 - Pr - 2r_2 + 4R\Delta t + 4Pr\phi\Delta t) \theta_i^j + \dots$$

$$(r_3 - Pr + r_2) \theta_{i+1}^j + r_5 (u_{i+1}^j - u_{i-1}^j)^2$$

(15)

$$-r_1 C_{i-1}^{j+1} + (Sc + 2r_1) C_i^{j+1} - r_1 C_{i+1}^{j+1} = -r_2 C_{i-1}^j + (Sc + Scr_4 - 2r_2) C_i^j + \dots$$

$$(r_2 - Scr_4) C_{i+1}^j - \Delta t Sc Kr (C_i^j)^2$$

(16)

From each one time Step, foremost the concentration and temperature field have been figured out, and so using the already known values of the concentration and temperature fields the velocity field is evaluated.

The action of computation is continuous till a steady state is neared by satisfying the following convergence criterion

$$\frac{\sum |A_{i,j+1} - A_{i,j}|}{M |A|_{\max}} < 10^{-5}$$

(17)

#### 4. Results and Discussion

To better perceive the flow rule, numeric figures for the velocity, temperature and concentration are plotted for variations of non-dimensional factors, such as the thermal Grashof number ( $Gr$ ), solutal Grashof number ( $Gc$ ), Magnetic field parameter ( $M$ ), viscoelastic parameter ( $Rm$ ), radiation parameter ( $R$ ), viscous dissipation parameter ( $Ec$ ) and Prandtl number ( $Pr$ ). The appropriate similarity variables have been provided, which converts the momentum and energy equations into a couple of nonlinear ordinary differential equations, hence simplifying the governing partial differential equations into ordinary differential equations. The finite difference approach was then used to achieve the numerical results. The analysis of the parameters

$Gr, Gc, M, k, R, Pr, \phi, Ec, Sc, Kr,$  and  $n$  effects on the velocity, temperature and concentration distributions were derived from the data. The impact of these factors on local Sherwood number, non-dimensional heat transfer coefficient and skin friction is also probed graphically.

Figures 1 and 2 are displayed to see the influence of thermal Grashof number and solutal Grashof number. From these plots, it is apparent that rising both thermal Grashof number and solutal Grashof number values cause the velocity across the boundary layer to rise. Figures 2 and 3 are depicted to see the consequences of viscoelastic parameter ( $Rm$ ) and magnetic field parameter ( $M$ ) on the velocity profiles. From this plot, it is evident that rising viscoelastic parameter ( $Rm$ ) values cause the velocity across the boundary layer to rise. This implies that the fluid flow velocity increases as the viscoelastic parameter increases. This practically points that the characteristics of fluid flow in viscoelastic fluids may be influenced by modifying the change in the  $K$ . For various values of the magnetic parameter ( $M$ ) the variation of the velocity distribution is shown in Figure 4. This shows that increasing the values of the magnetic parameter is a result of strengthening the values of  $M$ . This implies that when the magnetic field's strength increases, the fluid flow will face significant resistance or drag. This happens because a higher magnetic field causes a Lorenz drag, which raises the value of the drag force. In practice, this means that raising the intensity of the magnetic field might be used to limit the fluid flow rate, which could be a beneficial method for managing the final qualities of

the extrusion properties. Figure 5(a) and (b) displays the futures of radiation parameter ( $R$ ) with the velocity and temperature profile. It is observed from these graphs that the thermal field increased with the increase in  $R$ . More heat is transferred to the working liquid via the radiation phenomena because the radiation parameter is inversely related to the mean absorption coefficient. A higher radiation parameter value causes  $k^*$  to decline, which raises the temperature. As a result, the rate of thermal convection into the fluid increases, as does the deviation of radiative heat flow. The increased thermal heat transfer is advantageous for the development of thermal boundary layers. As a result, the thermal layer thickens. The course of the Prandtl number ( $Pr$ ) on the velocity and temperature profiles are seen in Figure 6(a) and (b). It is noticed that both velocity and temperature distribution diminishes. Fluids experience both conduction and convection. They can be viewed as competing with one another in terms of transmitting heat because the temperature differential is decreased by both processes, which transfer heat. If a fluid is more viscous, the Prandtl number is higher and the heat transfer will be less convective since  $Pr$  is the ratio of momentum to thermal diffusivity. The thermal boundary layer thickness and temperature distribution are reduced as a result of poorer thermal diffusivity, which is associated with larger values of  $Pr$ . As examined in Figures 7(a) and (b), a high value for the heat generation parameter amends the velocity field and the temperature field simultaneously. Heat production is represented by positive signs, and heat absorption is represented by negative signs. If we look at it from a physical standpoint, a heat source is anything that generates heat from the surface, which in turn raises the temperature of the fluid. Figure 8(a) and (b) displays the variation of viscous dissipation which is represented in terms of Eckert number  $Ec$  on the velocity and temperature profile. When a fluid is heated, viscous dissipation ( $Ec > 0$ ) causes the velocity and temperature to rise, however when a fluid is cooled, we see the opposite behaviour regarding the temperature profile when ( $Ec < 0$ ). On the other hand, due to the effect of viscous dissipation, the existence of viscous dissipation in the energy equation works as an internal heat source, causing the dimensionless temperature to increase at  $Ec > 0$  in comparison to  $Ec < 0$ . Due to frictional heating,  $Ec$  produces more heat in the liquid when it is physically more prominent. Consequently, a boost in velocity and temperature is assured. The velocity and concentration profile with

various Schmidt number ( $Sc$ ) values is graphed in Figure 9(a) and (b). As ( $Sc$ ) values grow, it is seen that the velocity and concentration distribution contracts. This is as result of increasing Schmidt number ( $Sc$ ) values strengthening the viscous force acting on fluid flow, it decreases the fluid flow velocity and concentration profile. For the varied parameter of the chemical reaction variable ( $Kr$ ), the distribution of both velocity and concentration profiles is illustrated in Figures 10(a) and (b). It has been remarked that when a chemical reaction's parameter values rise, the velocity and concentration profile inclines to descend. The existence of a chemical reaction parameter ( $Kr$ ), decays the velocity and concentration boundary layer's thickness by consuming the species and reducing fluid velocity and concentration. Figures 11(a) and (b) displayed that the rise in velocity and concentration curves when the order of chemical reaction parameter ( $n$ ) are high. As a result, the boundary layer thickness is increased in both cases

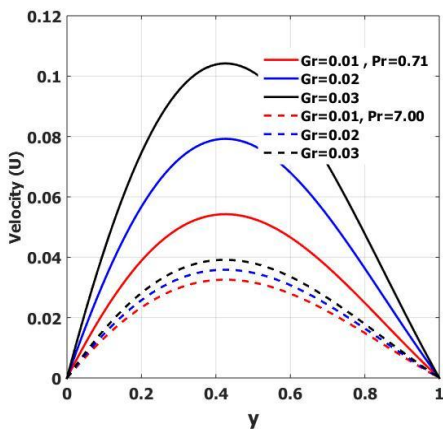


Figure 1: Impact of thermal Grashof number ( $Gr$ ) on velocity profile

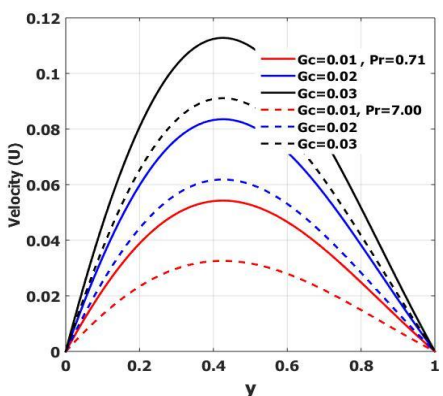


Figure 2: Impact of solutal Grashof number ( $Gc$ ) on velocity profile

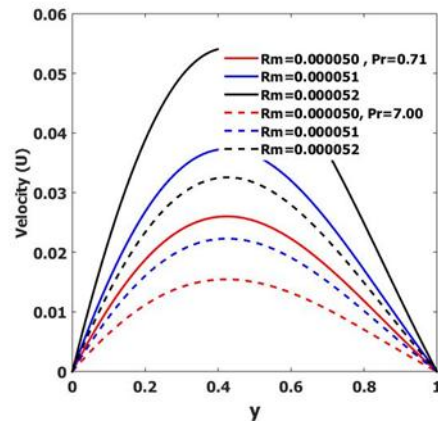


Figure 3: Impact of viscoelastic parameter ( $Rm$ ) on velocity profile

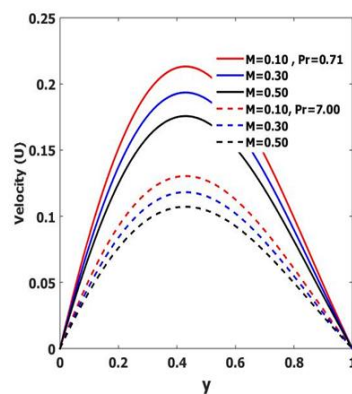


Figure 4: Impact of magnetic parameter ( $M$ ) on velocity profile

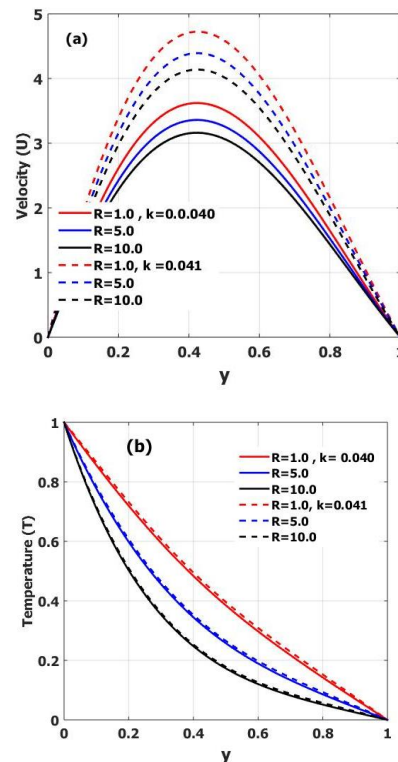


Figure 5: Impact of radiation parameter ( $R$ ) on velocity and temperature profiles

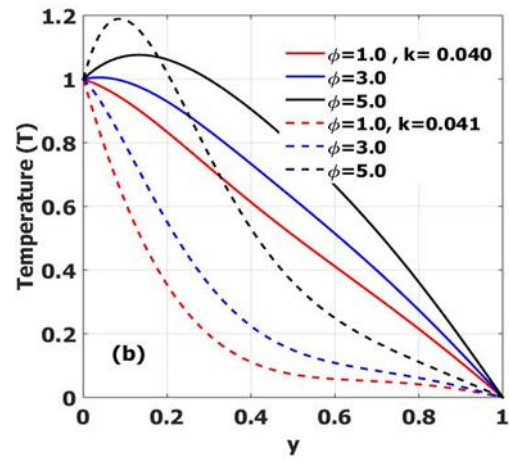
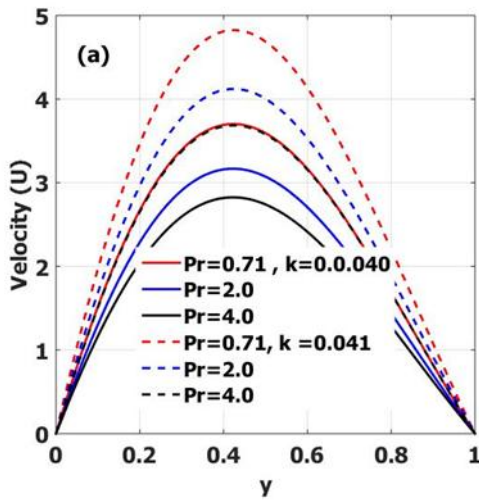


Figure 7: Impact of heat generation/absorption parameter ( $\phi$ ) on velocity and temperature profiles

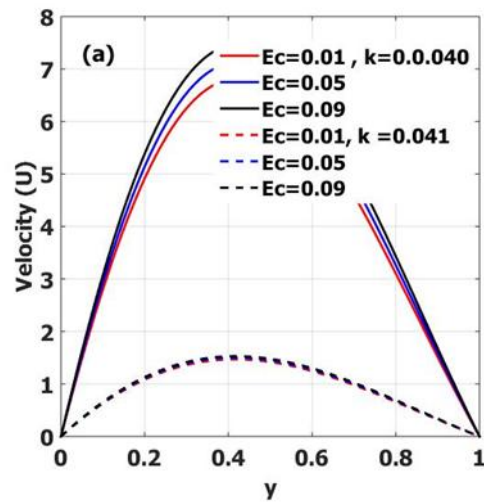
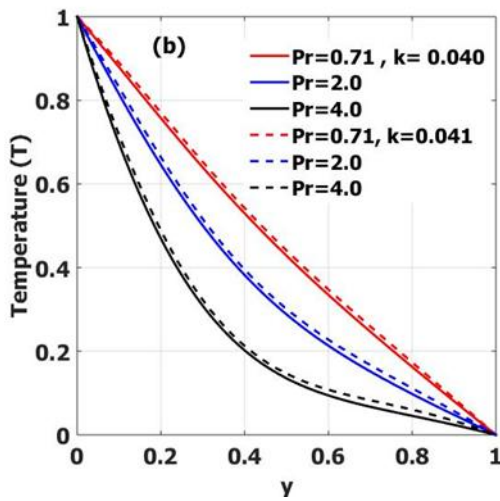


Figure 6: Impact of Prandtl number ( $Pr$ ) on velocity and temperature profiles

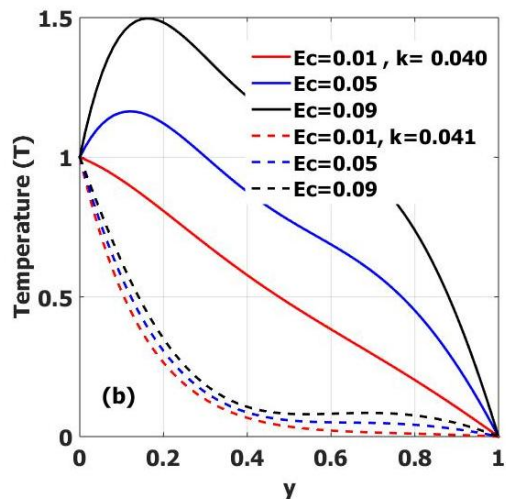
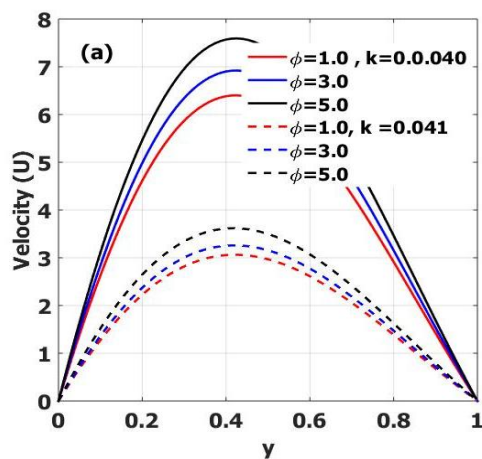


Figure 8: Impact of Eckert number ( $Ec$ ) on velocity and temperature profiles

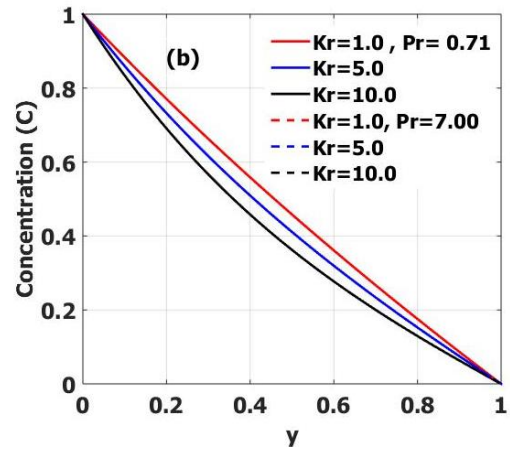
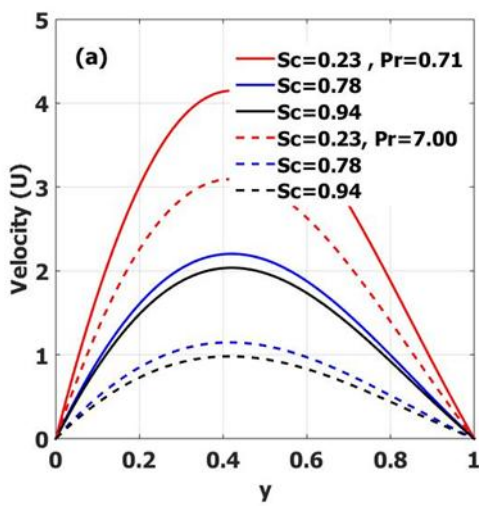


Figure 10: Impact of chemical reaction parameter ( $Sc$ ) on velocity and concentration profiles

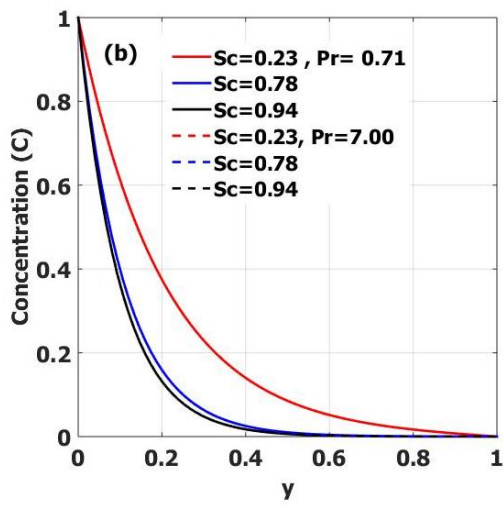


Figure 9: Impact of Schmidt number ( $Sc$ ) on velocity and concentration profiles

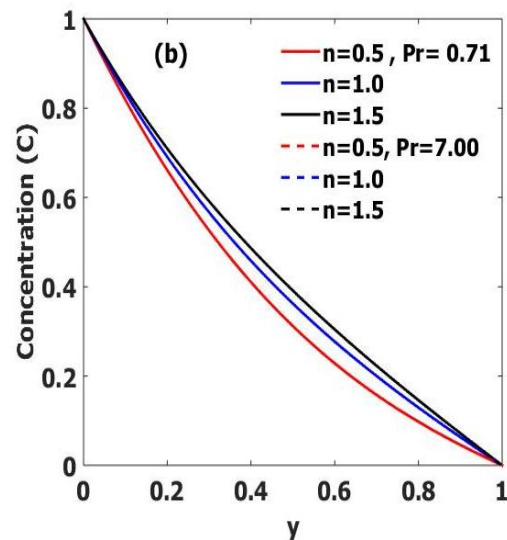
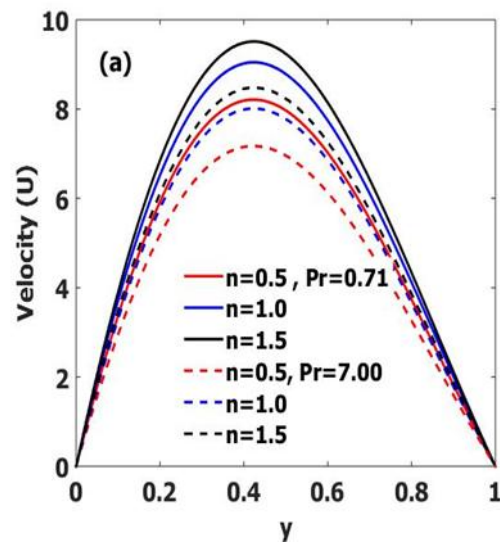


Figure 11: Impact of order reaction parameter ( $n$ ) on velocity and concentration profiles

The effect of viscoelastic parameter with respect to the magnetic field on skin friction is depicted in

Figure 12 (a) and (b). Relatively for smaller values of viscoelastic parameter the skin friction decreases. It is further observed that as magnetic field is altered the skin friction decreases as shown in Figure 12(a) and (b). at the plate  $y = 0$  and  $y = 1$ . The impact of magnetic field parameter on skin friction is shown in Figure 13(a) and (b). It is realized as magnetic field parameter grows skin friction decays. However, as porosity parameter increases skin friction increases. The effect of radiation parameter with reference to Prandtl number is exhibited in Figure 13(a) and (b). In general it seen that as the radiation parameter increases, the Nusselt number is found to be increasing. Is also deduced from the Figures that increasing Prandtl, increases the Nusselt number as seen in Figure 13(a). The reverse is the case in Figure 13(b). The effect of radiation parameter with reference to heat generation/absorption is pictured

in Figure 14(a) and (b). It is shown that as radiation parameter increases the Nusselt number also increases. It is further deduced that as heat generation/absorption parameter increases, Nusselt number increase.

The effect of Schmidt number with reference to chemical reaction parameter is examined in Figure 16(a) and (b). It is shown that as Schmidt number increases the Sherwood number also increases. It is further deduced that as chemical reaction parameter increases, Sherwood number increase. The effect of Schmidt number with reference to order of reaction parameter is examined in Figure 17(a) and (b). It is shown that as Schmidt number increases the Sherwood number also increases. It is further deduced that as reaction order parameter increases, Sherwood number increase.

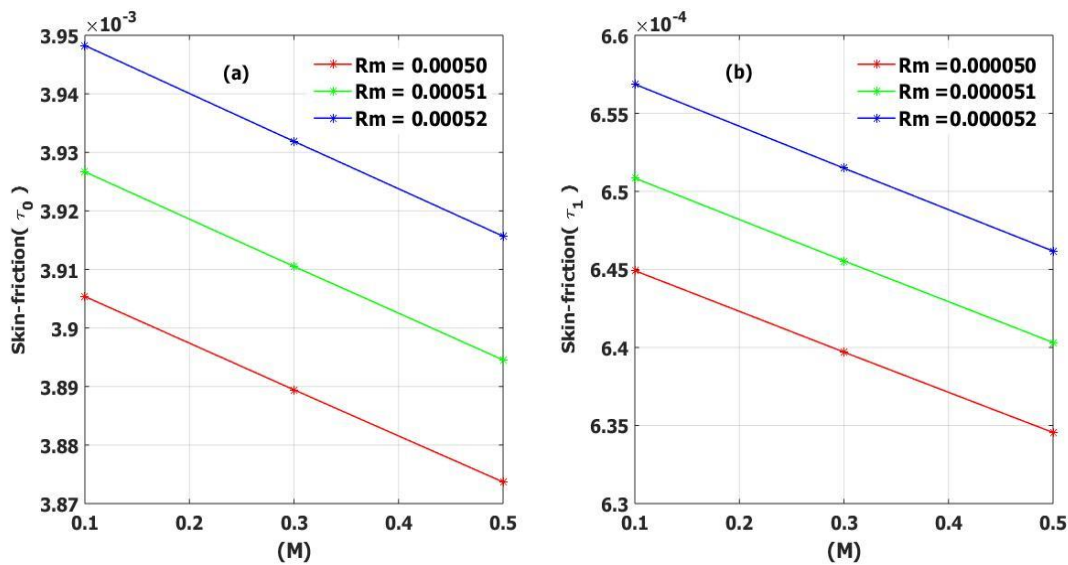


Figure 12: Impact of Skin friction ( $Sk$ ) against magnetic parameter

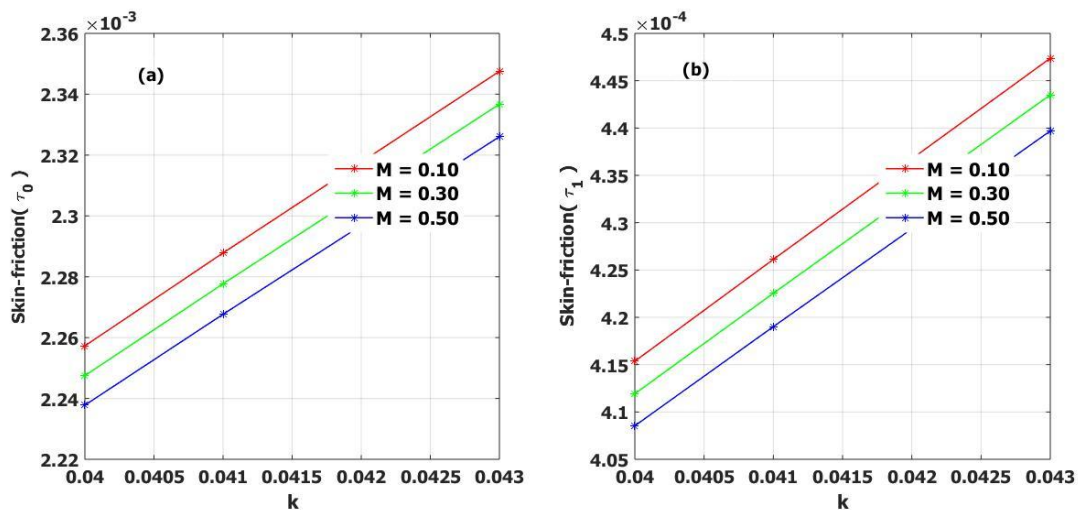


Figure 13: Impact of Skin friction ( $Sk$ ) against porosity parameter

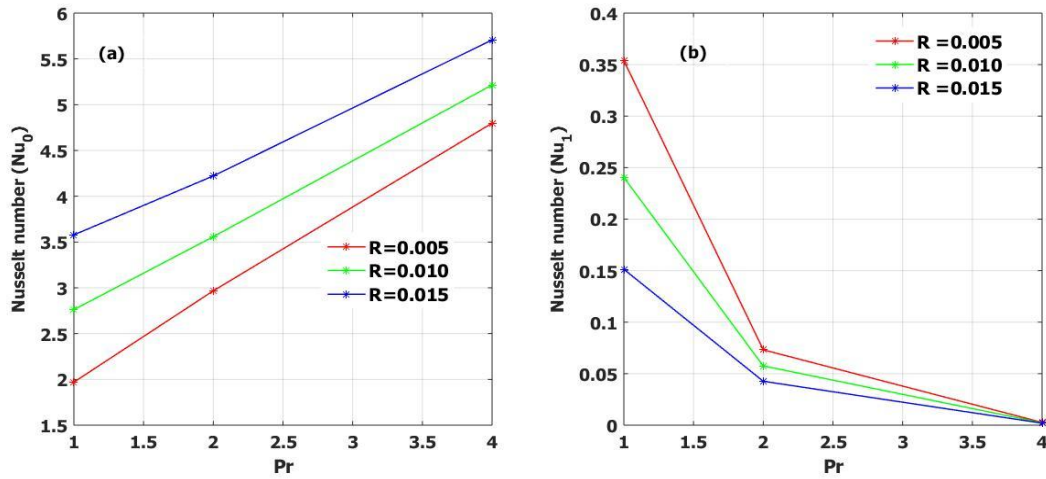


Figure 14: Impact of Nusselt ( $Nu$ ) against prandlt number

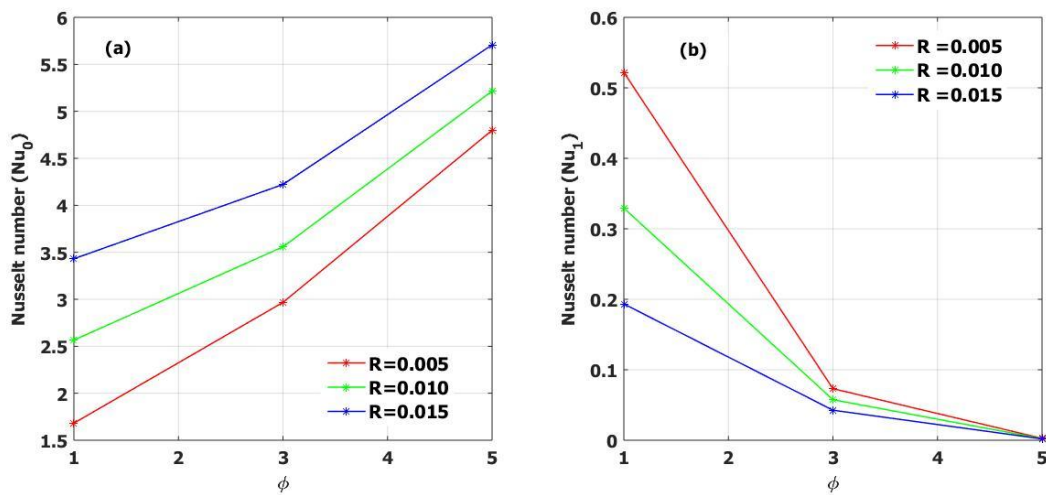


Figure 15: Impact of Nusselt number ( $Nu$ ) against heat generation/absorption parameter

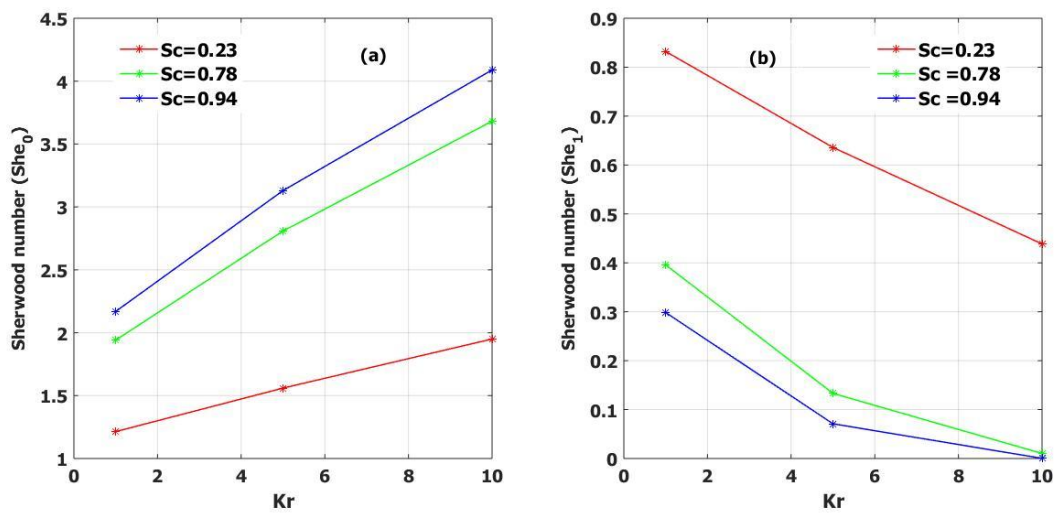


Figure 16: Impact of Sherwood number ( $Sh$ ) against chemical reation parameter

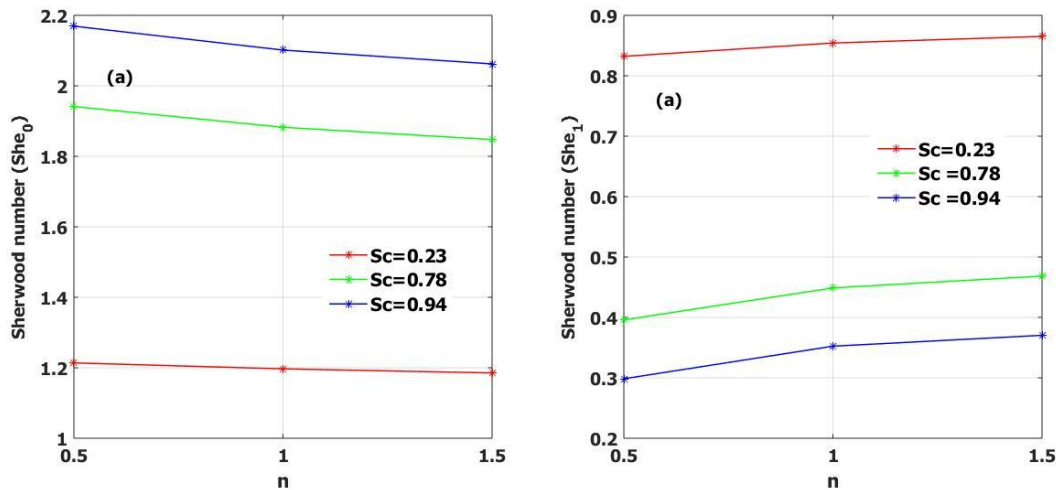


Figure 16: Impact of Sherwood number ( $Sh$ ) against order of reaction parameter

#### 4. Conclusion

In the presence of an applied magnetic field, thermal radiation, and viscous dissipation, the mathematical model including mixed convection boundary layer flow of viscoelastic fluid and heat transfer phenomena across a parallel plate has been investigated. When building heat transfer systems for diverse industrial applications, the rate of heat transmission is a key consideration. Depending on the applications, it may occasionally be necessary to increase or decrease the heat transfer rate to achieve better outcomes in the heating or cooling operations. Additionally, the findings are important since the material qualities of the wall rely on the pace of cooling or heating during the production of metal or polymer sheets. Therefore, an increase in temperature distribution and the associated thermal layer is caused by radiative and viscous dissipation. In reality, radiation causes more heat to be produced in liquids, raising their temperature. Radiation has an impact on heat transport and temperature distribution at high temperatures. Within the nonlinearly expanding boundary layer, opposing transport phenomena are where the magnetic field dominates. The study also shows that the applied magnetic field parameter increases the temperature profile while decreasing the rate of heat transfer through the walls. The results also showed that the increment of the nonlinear stretching sheet parameter  $n$  increases the drag coefficient due to an improvement in momentum diffusivity, which is the cause of the low rate of heat transfer because the rate of heat transfer decreases with increasing boundary layer thickness.

#### Conflict of interest

The authors declare no conflict of interest.

#### References

- O.D. Makinde, Free convection number flow with thermal radiation and mass transfer past a moving vertical porous plate, *Int. Commun. Heat Mass Tran.* 32 (10) (2005) 1411e1419, <https://doi.org/10.1016/j.icheatmasstransfer.2005.07.005>.
- T. Hayat, Z. Abbas, I. Pop, S. Asghar, Effects of radiation and magnetic field on the mixed convection stagnation-point flow over a vertical stretching sheet in a porous medium, *Int. J. Heat Mass Tran.* 53 (1e3) (2010) 466e474, <https://doi.org/10.1016/j.ijheatmasstransfer.2009.09.010>.
- S. Mukhopadhyay, K. Bhattacharyya, G.C. Layek, Steady boundary layer flow and heat transfer over a porous moving plate in presence of thermal radiation, *Int. J. Heat Mass Tran.* 54 (13e14) (2011) 2751e2757, <https://doi.org/10.1016/j.ijheatmasstransfer.2011.03.017>.
- K. Das, Impact of thermal radiation on MHD slip flow over a flat plate with variable fluid properties, *Heat Mass Tran.* 48 (5) (2012) 767e778, <https://doi.org/10.1007/s00231-011-0924-3>.
- S. Pramanik, Casson fluid flow and heat transfer past an exponentially porous stretching surface in presence of thermal radiation, *Ain Shams Eng. J.* 5 (1) (2014) 205e212, <https://doi.org/10.1016/j.asej.2013.05.003>.
- H.R. Kataria, H.R. Patel, Soret and heat generation effects on MHD Casson fluid flow past an oscillating vertical plate embedded through porous medium, *Alex. Eng. J.* 55 (3) (2016)

- 2125e2137, <https://doi.org/10.1016/j.aej.2016.06.024>.
- M. Sheikholeslami, M.M. Rashidi, Non-uniform magnetic field effect on Nano fluid hydrothermal treatment considering Brownian motion and thermophoresis effects, *J. Braz. Soc. Mech. Sci. Eng.* 38 (4) (2016) 1171e1184, <https://doi.org/10.1007/s40430-015-0459-5>.
- C. Sulochana, S.S. Payad, N. Sandeep, Non-uniform heat source or sink effect on the flow of 3d Casson fluid in the presence of Soret and thermal radiation, *Int. J. Eng. Res. Afr.* 20 (2016) 112e129, <https://doi.org/10.4028/www.scientific.net/JERA.20.1>
- G. Kumaran, N. Sandeep, Thermophoresis and Brownian moment effects on parabolic flow of MHD Casson and Williamson fluids with cross diffusion, *J. Mol. Liq.* 233 (2017) 262e269, <https://doi.org/10.1016/j.molliq.2017.03.031>.
- C. Sulochana, S.S. Payad, N. Sandeep, Non-uniform heat source or sink effect on the flow of 3d Casson fluid in the presence of soret and thermal radiation, *Int. J. Eng. Res. Afr.* 20 (2016) 112e129, <https://doi.org/10.4028/www.scientific.net/JERA.20.112>.
- D. Mythili, R. Sivaraj, Influence of higher order chemical reaction and nonuniform heat source/sink on Casson fluid flow over a vertical cone and flat plate, *J. Mol. Liq.* 216 (2016) 466e475, <https://doi.org/10.1016/j.molliq.2016.01.072>.
- E.K. Ghiasi, R. Saleh, 2d flow of Casson fluid with nonuniform heat source/sink and joule heating, *Frontiers in Heat and Mass Transfer (FHMT)* 12 (2019) 1e7, <https://doi.org/10.5098/hmt.12.4>.
- P.D. Prasad, S. Saleem, S.V.K. Varma, C.S.K. Raju, Three-dimensional slip flow of a chemically reacting Casson fluid flowing over a porous slender sheet with a non-uniform heat source or sink, *J. Kor. Phys. Soc.* 74 (9) (2019) 855e864, <https://doi.org/10.3938/jkps.74.855>.
- M. Yasir, A. Ahmed, M. Khan, A.K. Alzahrani, Z.U. Malik, A.M. Alshehri, Mathematical modelling of unsteady Oldroyd-B fluid flow due to stretchable cylindrical surface with energy transport, *Ain Shams Eng. J.* 14 (1) (2023) 101825, <https://doi.org/10.1016/j.asej.2022.101825>.
- M. Yasir, A. Ahmed, M. Khan, M.Z. Ullah, Convective transport of thermal and solutal energy in unsteady MHD Oldroyd-B Nano fluid flow, *Phys. Scripta* 96 (12) (2021) 5266, <https://doi.org/10.1088/1402-4896/ac3b67>.
- Abel, S. Heat transfer in MHD viscos-elastic fluid flow over a stretching surface. *ZAMM J. Appl. Math. Mech.* 81(10), 691–698 (2001).
- Sivaraj, R. & Kumar, B. R. Viscoelastic fluid flow over a moving vertical cone and flat plate with variable electric conductivity. *Int. J. Heat Mass Transf.* 61, 119–128 (2013).
- Maryam, A. N., Ali, B., Moghadam, J. & Norouzi, M. A numerical study on viscoelastic boundary layer on flat plate. *J. Braz. Soc. Mech. Sci. Eng.* 42(1), 11 (2020).
- Cortell, R. A novel analytic solution of MHD flow for two classes of viscos-elastic fluid over a sheet stretched with non-linearly (quadratic) velocity. *Meccanica* 48(9), 2299–2310 (2013).
- Mustafa, M. Viscoelastic flow and heat transfer over a non-linearly stretching sheet: OHAM solution. *J. Appl. Fluid Mech.* 9, 1321–1328 (2016).
- Hayat, T., Qayyum, S., Alsaedi, A. & Ahmad, B. Magnetohydrodynamic (MHD) nonlinear convective flow of Walters-B Nano fluid over a nonlinear stretching sheet with variable thickness. *Int. J. Heat Mass Transf.* 110, 506–514 (2017).
- Kumaran, G., Sivaraj, R., Prasad, V. R., Beg, O. A. & Sharma, R. P. Finite difference computation of free magneto-convective Powell-Eyring Nano fluid flow over a permeable cylinder with variable thermal conductivity. *Phys. Scr.* 96(2), 025222 (2000).
- Yaseen, M., Rawat, S. K. & Kumar, M. Hybrid Nano fluid (MoS<sub>2</sub>–SiO<sub>2</sub>/water) flow with viscous dissipation and Ohmic heating on an irregular variably thick convex/concave-shaped sheet in a porous medium. *Heat Transfer* 51(1), 789–817 (2022).